



ASME Accepted Manuscript Repository

Institutional Repository Cover Sheet

Cranfield Collection of E-Research - CERES

ASME Paper

Title: A marine turbocharger retrofitting platform

Authors: Konstantinos Ntonas, Nikolaos Aretakis, Ioannis Roumeliotis, Konstantinos Mathioudakis

ASME Journal

Title: Journal of Engineering for Gas Turbines and Power

Volume/Issue: Volume 142, Issue 11, Paper GTP-20-1402 Date of Publication (VOR* Online) 2 October 2020

ASME Digital Collection URL: <https://asmedigitalcollection.asme.org/gasturbinespower/article/142/11/111008/1087606/A-Marine-Turbocharger-Retrofitting-Platform>

DOI: <https://doi.org/10.1115/1.4048652>

*VOR (version of record)

A MARINE TURBOCHARGER RETROFITTING PLATFORM

Konstantinos Ntonas
Research Assistant
kntonas@central.ntua.gr

Nikolaos Aretakis
Assistant Professor
naret@central.ntua.gr

Ioannis Roumeliotis
Research Associate
I.Roumeliotis@cranfield.ac.uk

Konstantinos Mathioudakis
Professor
kmathiou@mail.ntua.gr

Laboratory of Thermal Turbomachines, School of Mechanical Engineering
National Technical University of Athens, Athens, Greece

ABSTRACT

A turbocharger retrofitting platform utilizing 1D models for calculating turbomachinery components maps and a fully coupled process for integration with the turbomachinery components and the diesel engine, is presented. The platform has been developed with two modes of operation, allowing the retrofitting process to become fully automatic. In the first mode, available turbo-components are examined, in order to select the one that best matches the entire engine system, aiming to retain or improve the diesel engine efficiency. In the second mode, an optimization procedure is employed, in order to redesign the compressor to match the entire system in an optimum way. Dimensionless parameters are used as optimization variables, for a given compressor mass flow and power.

A retrofitting case study is presented, where three retrofitting options are analyzed (compressor retrofit, turbocharger retrofit and compressor redesign). In the first and second option, turbocharger retrofitting is carried out, using available turbo-components. It is shown that initial performance cannot be reconstituted using off-the-self solutions. In the third option, compressor designing is performed, using the optimization mode, in order to provide an improved retrofitting solution, aiming to at least reconstituting the original diesel engine performance. Finally, a CFD analysis is carried out, in order to validate the compressor optimization tool capability to capture the performance trends, based on geometry variation.

NOMENCLATURE

Abbreviations

CFD	Computational Fluid Dynamics
IC	Internal Combustion
OTE	Original Turbocharged Engine
T/C	Turbocharger

Symbols

A	Area	[m ²]
C	Speed of Sound	[m/s]

C_p	Specific heat ratio	[kJ/kg K]
D_h	Specific enthalpy change	[kJ/kg]
N_s	Specific Speed	[-]
\dot{m}	Mass flow rate	[kg/s]
MN	Mach number	[-]
N	Speed	[Rpm]
P	Pressure	[Pa]
PR	Pressure ratio	[-]
P_{wr}	Power	[kW]
R	Impeller radius	[m]
R_{gas}	Air gas constant	[kJ/kg K]
S	Dimensionless distance between leading and trailing edge	[-]
S_{fc}	Specific Fuel Consumption	[g/kWh]
T	Temperature	[K]
t_c	Blade thickness	[mm]
U	Blade speed	[m/s]
V	Absolute velocity	[m/s]
Z	Impeller full blade number	[-]

Greek Letters

β	Blade angle	[deg]
η	efficiency	
σ	Slip factor	[-]
ρ	Density	[kg/m ³]
Φ	Flow coefficient	[-]
ω	Angular velocity	[rad/s]

Subscripts

1	Impeller inlet
1h	Impeller inlet hub

<i>1t</i>	Impeller inlet tip
<i>1m</i>	Impeller inlet mid
<i>2</i>	Impeller outlet
<i>3</i>	Vaneless diffuser outlet
<i>a</i>	Axial
<i>AD</i>	Adiabatic
<i>comp</i>	Compressor
<i>d</i>	Design
<i>cor</i>	Corrected
<i>dl</i>	Diffuser loss
<i>DF</i>	Disk friction
<i>ex</i>	External-parasitic
<i>le</i>	Leading edge
<i>m</i>	mechanical
<i>r</i>	Radial
<i>RC</i>	Recirculation
<i>s</i>	Static conditions
<i>t</i>	Total conditions
<i>te</i>	Trailing edge
<i>turb</i>	Turbine
<i>U</i>	Circumferential

INTRODUCTION

Turbocharged internal combustion (IC) engines have been widely used in vehicles, heavy duty trucks, ships, non-interconnected small electric power systems and other small energy applications. In particular, these engines have a leading role in marine industry, used either as main engines or as auxiliary power generator-sets (GENSETS) [1].

As discussed by Button et al [2], the main contributors in the life cycle cost of the turbocharged IC engines are maintenance and operational costs. Both costs increase as turbocharger (T/C) degradation occurs due to the harsh working conditions, leading to frequent turbo-components replacements. In many cases of an aged T/C not available anymore in the market, retrofit is performed, by replacing specific component (compressor or turbine) or entire T/C with a new one available in the market.

The T/C retrofit is a complicated and time consuming process, due to the fact that each turbo-component must be chosen carefully, in order to match the IC Engine, while retaining or improving the whole system efficiency. The automatization of such a process can benefit both T/C manufacturer and marine company, by decreasing the retrofitting process time, hence leading to lower process cost, productivity improvement and anchored ship time reduction. For the majority of retrofitting cases, the most obvious approach is to use market available turbo-components, because of the high cost of new component designing and manufacturing. In case of no available component that suitably matches the IC engine, a possible step is the redesigning of a new geometry, able to match the diesel engine. A lot of T/C manufactures focus on compressor, using available turbine if it is possible, because as Watson and Janota mention [3], “the T/C turbine can operate efficiently over a wider mass flow range than its compressor”. Designing and modeling of a centrifugal compressor is performed using 1D or 3D analysis. For 1D analysis, used in the current work, a component performance map calculation is carried out with geometrical parameters as input data.

This analysis calculates the off-design performance using a mean streamline single zone model [4, 5]. Rodgers [6] tried to set the surge and choke limits for a wide range of centrifugal compressors using experimental data. Another contribution to the 1D model was made by Japikse [7], who assumed that the jet-wake structure exists in the impeller passage. A different approach was made by Stuart et al [8,9] who developed the three zone model by showing that impeller exit recirculation influences compressor work input.

In the present work, Galvas [4] single zone centrifugal compressor mean line code is used, employing Rodgers [6] correlations for surge and choke limits prediction. Stuart et al [8,9] is used in order to develop an empirical correlation for calculating the exducer to inducer area ratio based on impeller flow coefficient.

Geometry optimization is always sought in centrifugal compressor design process. Rossetti et al [10] focused on vaned diffuser with incompressible flow optimization, trying to achieve the best compromise between flow deflection, static pressure recovery and total pressure loss. Li et al [11] on the contrary created an optimization design method for the whole centrifugal compressor, using 1D single zone model. The second part of his work focused on impeller and vaned diffuser matching optimization. The above researchers propose an optimization procedure using geometrical parameters as variables. Thus, it cannot be automated due to the fact that it is not robust in case of random initial geometry usage.

In the present study a novel marine turbocharger retrofitting platform has been developed. It utilizes 1D models for calculating the turbomachinery components maps and a 1D fully coupled process integrating the turbomachinery components and the diesel engine. It has two modes of operation which aim to make retrofit process fully automatic, fast and reliable, either by choosing the best fitted turbo-component, or by redesigning it through an optimization process. The second mode provides a robust solution independent of initial data, by using dimensionless parameters as variable. Thus, it allows the initialization with random values, hence making the optimization mode fully automatic. Furthermore, for compressor redesigning, a 3D geometry is generated,

utilizing a transformation from 1D to 3D geometry technique, developed in the context of the present work. Finally, the platform, suggests the best solution based on estimated cumulative benefit in function of time of operation, after analyzing all three retrofit options (compressor replacement, entire turbocharger replacement and compressor redesign).

Validation of the model of each individual component, namely compressor 1D model, turbine 1D model and diesel single zone model, as well as the entire turbocharged diesel engine, has been performed. The validation has been extensively described in another publication of the group of the authors (Ntonas et al) [12]. The platform is applied to a retrofitting test case for a diesel engine operating in the field. Application of all three retrofit options is examined.

TURBOCHARGER RETROFITTING PLATFORM

The simulation framework utilizes 1D models for calculating the turbomachinery components maps and then a fully coupled process integrating the turbomachinery components. The T/C is connected to a diesel engine and an intercooler as shown in Figure 1, allowing the calculation of the performance and operating conditions at sub-system and system level.

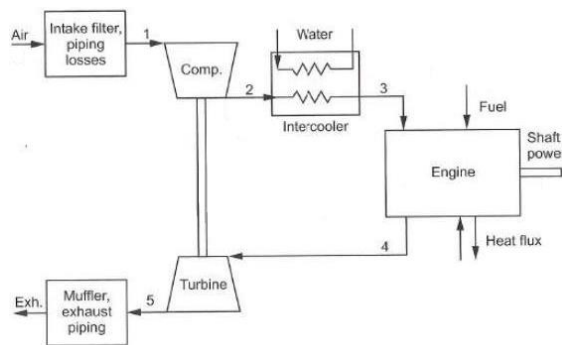


Figure 1: Turbocharged diesel engine layout.

Compressor and turbine models are based on the methodology presented by Galvas [4] and Wasserbauer [13] respectively. For the diesel engine, an in-house single zone thermodynamic combustion model has been used for the closed engine cycle, with the capability of being calibrated based on available shop trials data, hence improving prediction accuracy.

In order to ensure the applicability of the above presented framework in capturing turbocharged diesel engine operation, a validation process has been carried out. Validation of the model of each individual component, namely compressor 1D model, turbine 1D model and diesel single zone model as well as the entire turbocharged diesel engine has been performed. The validation has been extensively described in another publication of the group of the authors (Ntonas et al). [12].

By using both compressor and turbine models, a data-base is developed with 13 different turbocharger 1D geometries in order to be used during retrofit process. The turbochargers are from the production line of partner company. [14] For matching criteria, turbocharger must provide the necessary boost pressure, in order for the IC Engine to generate the demanded nominal power. Ideally,

the turbo-components operating nominal points should be in high efficiency area. In addition compressor operating line distance from surge line must be as large as possible [15]. The degree of fulfilling these criteria is indicative of matching quality.

Turbocharger retrofit using available turbo-components (Mode 1)

The platform first mode of the platform provides an automatic T/C retrofit choice. By examining all turbo-components (compressors and turbines) available in data base, it selects the one that best matches the entire engine system, aiming to retaining or improving the diesel engine original efficiency, certified during shop trials.

It sorts the available turbo-components, the technical specifications of which are stored in a database, according to the matching quality and the calculated overall performance. Additionally, a capability of checking specific turbo-components as retrofitting parts is provided, leading to a high computational cost reduction, if specific original turbocharger component (e.g. turbine) is available.

In case that the optimum turbocharger does not fully satisfy the matching criteria, the platform also integrates flow trimming tool [16] for compressor or turbine that adapts the turbocharger performance in order to satisfy the matching requirements .

Vaneless diffuser Centrifugal Compressor Redesign (Mode 2)

In the second mode, an optimization procedure is followed, redesigning the compressor in order to match the entire system in an optimum way, retaining the original turbine. The usage of dimensionless parameters (e.g. N_s , Φ , etc.) gives, a robust and fast converging procedure is provided, without specific initial geometry requirement.

For making the optimization process fully automatic, constant variables ranges are imposed (Table 1) in order to satisfy every compressor performance requirement, while the initialization is performed using random values from the ranges shown.

Table 1: Dimensionless geometrical parameters.

Parameter	Range	Parameter	Range
Z	(6,40)	R_{1H}/R_{1T}	(0.25,0.70)
N_s	(0.45,1.25) [17]	MN_3	<0.95
Φ_2	(0.1,0.5)	β_2	(0,80)
R_{1T}/R_2	(0.3,0.8)		

The ranges have been calculated in cooperation with partner company [14], by examination of 13 turbocharger compressor geometries provided.

The usage of dimensionless parameters is achieved by coupling a typical compressor 1D mean line model [4] with a pre-processor, capable of transforming dimensionless parameters into 1D geometry as explained in the Appendix. This transformation is accomplished by using compressor mass flow and power as input data. Input and output data are the following:

- Input data: $P_{wr_{turb}}$, \dot{m} , Z , N_s , Φ_2 , R_{1T}/R_2 , R_{1H}/R_{1T} , MN_3 , β_2 ,
- Output data: R_{1h} , R_{1t} , R_2 , R_3 , b_2 , b_3 , Z , β_{1m} , β_2

The procedure followed is shown in Figure 2.

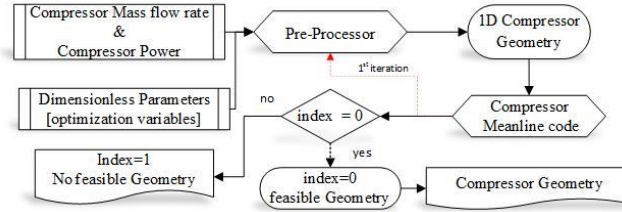


Figure 2: Compressor model flow chart.

The compressor model integrates restrictions that ensure physically acceptable solutions, while they reduce computational cost. The compressor optimization restrictions are given in Table 2.

Table 2: Optimization restrictions.

$\eta_{\text{comp,AD}}$	PR	MN_{1t}	\dot{m}_{cor}	N_{comp}
(0,0.94)	>1	<1.05	($\dot{m}_{\text{surge}}, \dot{m}_{\text{choke}}$)	= N_{turb}

By using an “index” parameter, compressor informs the optimizer about the solution feasibility. In case of hybrid T/C the restriction “ $N_{\text{comp}} = N_{\text{turb}}$ ” is not included. The blade thickness is not opted for optimization variable due to the lack of stress analysis. Thus, blade thickness is set, by using inducer rms blade blockage factor as a constant, equal to the 1D centrifugal compressor validation test case [4]. It should also be noted that, mode 2 is limited to vaneless diffuser centrifugal compressor redesigning.

For optimization method, a Multi-Objective Particle Swarm [18] and a Downhill Simplex technique are sequentially coupled. In the first iteration Multi-Objective Particle Swarm optimization is carried out, due to its ability to capture an optimum solution fast without the usage of a feasible initial geometry. Then, having the particle swarm solution as initial geometry, a Downhill Simplex technique is checking locally, if an efficiency improvement can be succeed. For Multi-Objective Particle Swarm optimization, the inertia is 0.721, the maximum velocity 250, the number of particles 35 and the particle increment 1.655. As for Downhill Simplex, an initial simplex size equal to 0.1 is chosen.

Modification of the single-zone model

The basic disadvantage of the single-zone model in contrast to three zone model, developed by Stuart et al [8,9], is its inability to calculate the impact of impeller outlet blade length in recirculation and active flow region generation. However, for the current work, the single zone model is chosen due to the fact that three zone model requires a series of CFD simulations for calculating the relationship between flow coefficient, specific speed and aerodynamic blockage. Thus, in the current optimization process, the impeller outlet blade length tends to be as large as it can. For overcoming this issue, an impeller outlet blade length restriction is developed. To elaborate further, using a number of compressor measured geometries, the compressor outlet to inlet area ratio is

calculated as a function of design flow coefficient, assuming that specific speed does not affect the aerodynamic blockage. A correlation is established as shown in Figure 3.

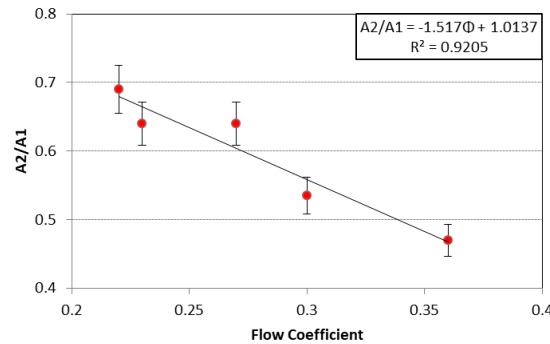


Figure 3: A_2/A_1 as a function of flow coefficient.

The negative trend is evident in accordance to Stuart et al work [9]. Thus, the following equation is implemented into the optimization procedure

$$A_2/A_1 = -1.51 \Phi + 1.0137 \quad (1)$$

A MARINE TURBOCHARGER RETROFITTING PLATFORM TEST CASE

The use of the platform is demonstrated through application of a retrofitting test case is presented, where the above described retrofitting platform is applied. Specifically, a turbocharged 5-cylinder 4-stroke diesel generator is to be retrofitted, following of a T/C vaneless diffuser compressor material failure. Shop trials data are available, allowing diesel engine model calibration. Three retrofit options are analyzed, aiming to guide the T/C manufacturer in opting for the most suitable one, based on system matching-performance and manufacturing economic analysis.

- Option 1: Compressor retrofit, using available compressors.
- Option 2: Entire turbocharger retrofit, using available compressor and turbine couples.
- Option 3: New turbocharger compressor design (compressor optimization).

Original Turbocharger Operation

For original turbocharger operation analysis, having measured and using as input the original T/C geometry, in combination with the available shop trials data, the calculation of turbocharged diesel engine operation is performed [12]. The calculated and the measured specific fuel consumption against engine power are presented in Figure 4 for five different operating points (Load: 25, 50, 75, 100 and 110%).

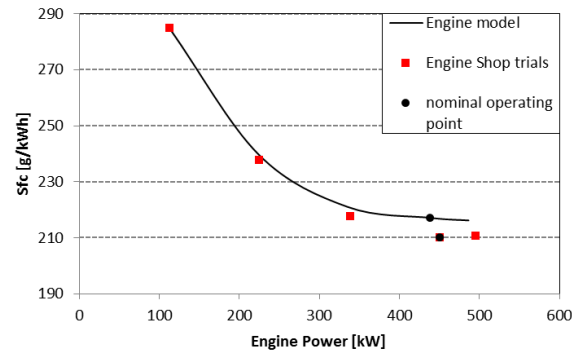


Figure 4: SFC against engine power.

It is shown that the proposed integrated model simulates the overall engine operation in very good agreement to the engine shop trials data. The maximum deviation from the reported mean sfc value is 2.6%. Performance maps (predicted by mean line codes) and operating lines are presented in Figure 5 and Figure 6 respectively.

Option 1: Compressor retrofit

Retrofit is performed by choosing a compressor individually, by using platform first mode while retaining the original turbine. The retrofitted compressor operating line is presented in Figure 7, showing the matching quality with the entire diesel engine system. The comparison to Figure 4 shows that the maximum turbocharger speed drops about 12%, hence positively affecting turbocharger life. A 0.8% increase in SFC at nominal operational point is also noticed (Figure 9). The retrofitted compressor is chosen from the inventory of available compressors, which already exists and have their corresponding performance characteristics. The platform makes the best choice among those, but even the most suitable one is not perfectly fitted for the given diesel engine. In order to have the possibility of optimum fitting the platform is equipped with Mode 2 (Option 3) that will be discussed further in the paper..

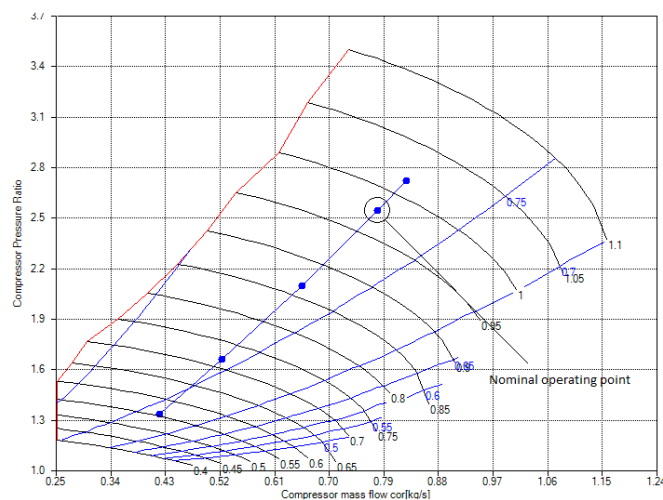


Figure 5: Original compressor map and operating line.

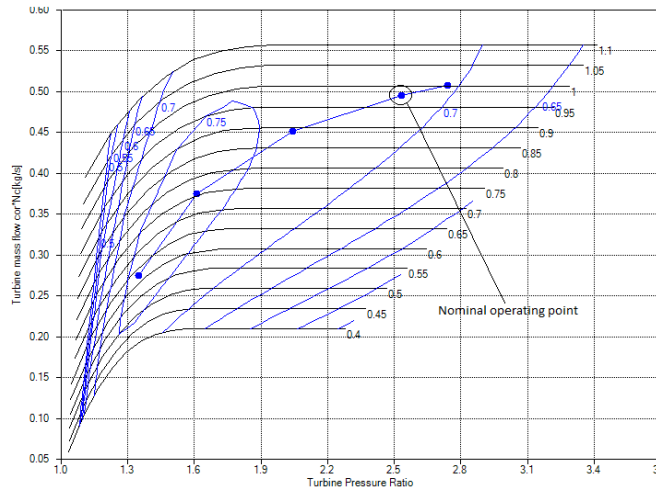


Figure 6: Original turbine map and operating line.

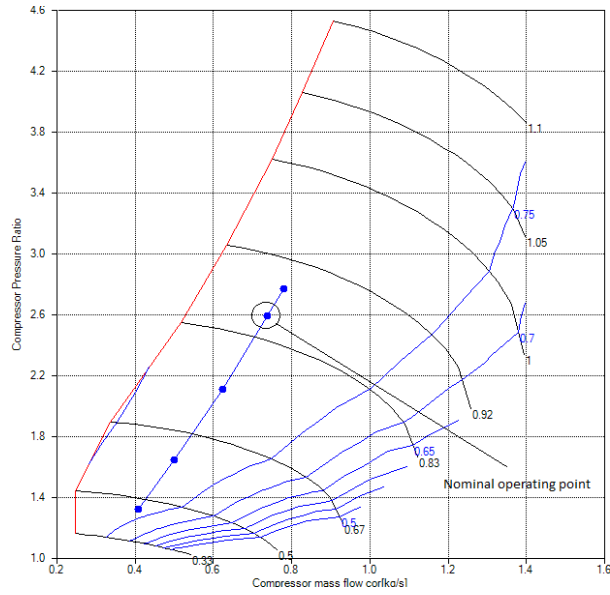


Figure 7: Retrofitted compressor map and operating line.

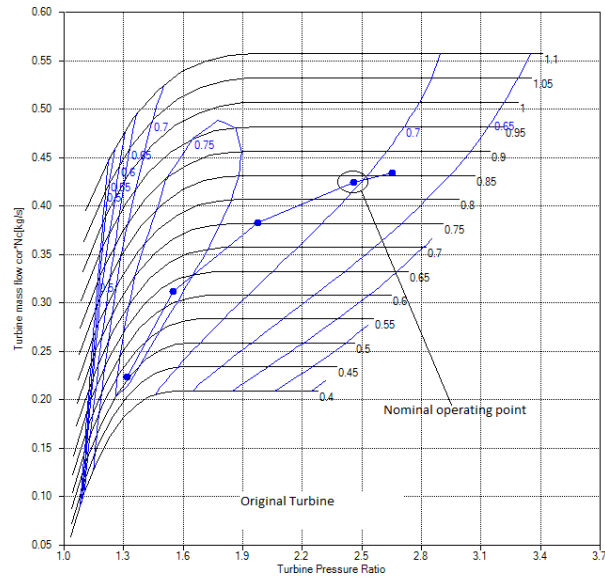


Figure 8: Original turbine map and operating line (option1).

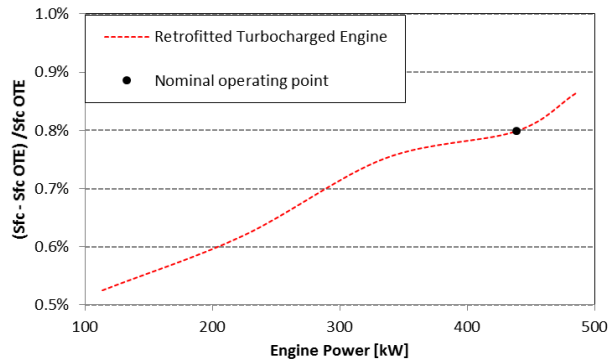


Figure 9: SFC change for retrofitted compressor.

For the sake of demonstrating further platform capabilities, a flow trimming process [16] is performed in the current compressor. This process by cutting compressor blade tip moves the surge line away from the operating line. This platform capability is applied in case that compressor operates close to surge line.

The performance maps for trimmed compressors by 5 and 10% along with T/C operating line are shown in Figure 10. Both trimmed compressors ensure the turbocharger stable operation and the matching quality between compressor and the entire diesel engine system.

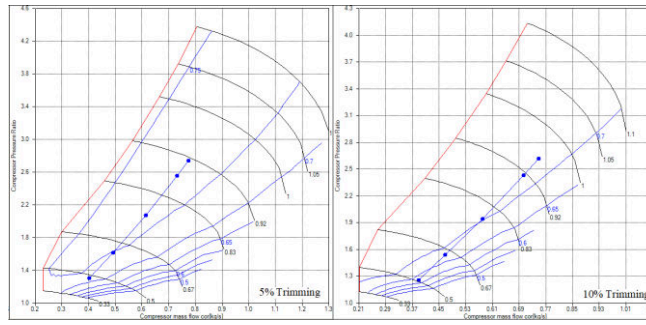


Figure 10: Trimmed compressor performance maps and operating lines.

The trimmed compressor by 5% is considered more appropriate because the specific fuel consumption increase is negligible compared to the 10%, as Figure 11 shows. Additionally, the turbocharger maximum speed is slightly higher by 5%, although having a maximum speed lower than design speed, hence not working in over-speed conditions.

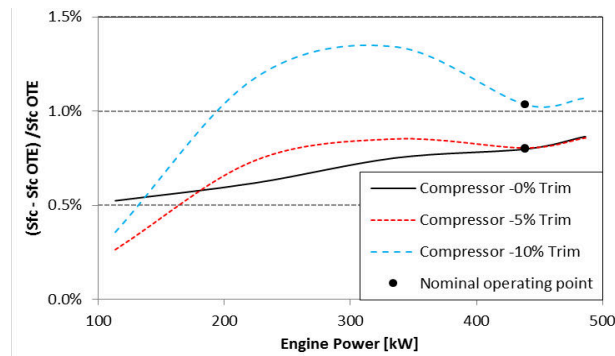


Figure 11: Sfc change for trimmed compressors retrofit.

Option 2: Entire turbocharger retrofit

In the second option, retrofit is carried out using entire T/C (compressor and turbine). The best fitted T/C is the one that consists of the compressor, chosen in option 1. The turbocharger speed does not exceed the design value, hence decreasing the chance of bearing failure due to over-speed. However, due to the turbine replacement, the maximum T/C speed increases about 11.37% (Figure 8 and

Figure 12). For the sfc line, a slight increase in nominal operating point about 0.27% is shown in Figure 13 which is similar to the option one. Thus, the weakness of the retrofit process using available turbo-components instead of redesigning the entire T/C is shown.

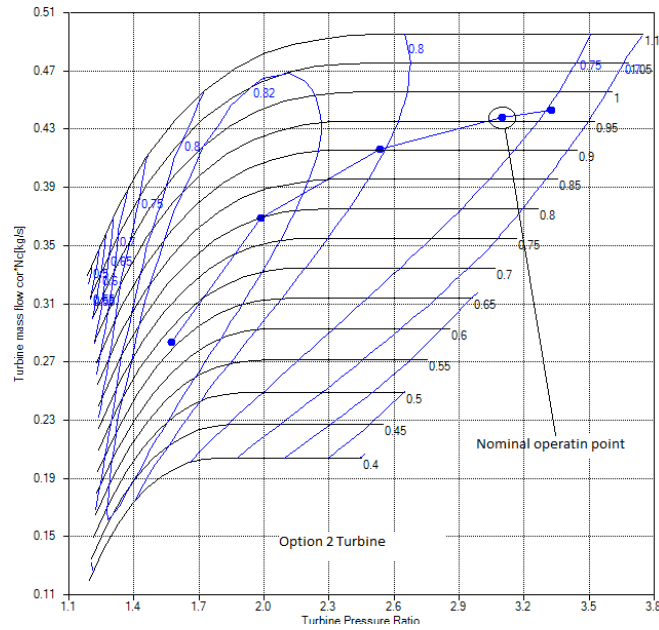


Figure 12: Option 2 turbine map and operating line.

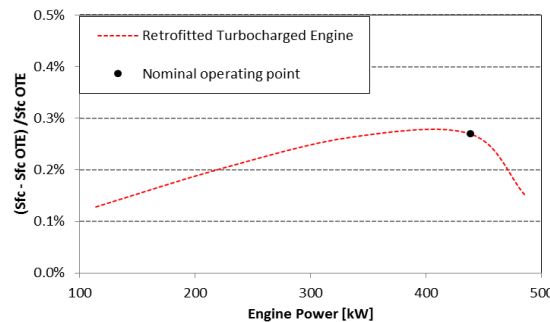


Figure 13: Sfc change for entire T/C retrofit.

To sum up, the current option provides a slightly better retrofitting solution (Figure 9 and Figure 13), having lower specific fuel consumption in comparison to Option 1. However, it should be noted that the replacement of entire turbocharger instead of a compressor increases the process cost, hence making Option 2 less attractive.

Option 3: New compressor design

In the third option, compressor designing is performed, using the optimization mode (second mode), in order to provide an improved retrofitting solution, aiming to at least reconstituting the original diesel engine performance, certified during shop-trials. For basic input data, the mass flow and the turbine power are used, which in the current case are available by the shop trials engine data. In particular, default values are used for optimization process initialization, noting that this process is fully automatic.

The restrictions, used in the current case, have been extensively presented in the previous section. Additional to these, an extra restriction is added, which is the hub radius. This restriction ensures that compressor can fit to specific diameter turbocharger axis.

The geometrical parameters differences between original and optimized compressor are shown in Table 3. Also main blade number decreases by one.

Table 3: Difference in geometry between original and optimized compressor.

R_{1H}/R_T	R_{1T}/R_2	A_2/A_1	Φ	β_{1M}	β_2
4%	10%	6%	12%	71%	37.8%

It is obvious that optimized compressor geometry has similar size to the original one, hence validating the right operation of the second mode, knowing that initialization is performed based on default values. For optimized compressor, Figure 14 and Figure 15 highlight the performance improvement in relation to original compressor. Specifically, a relative pressure ratio and absolute efficiency increase in nominal operating point of 12.39% and 2% respectively are achieved. The maximum absolute efficiency increase is about 3.8%, with a significant movement of design point about 34.6% (Figure 15).

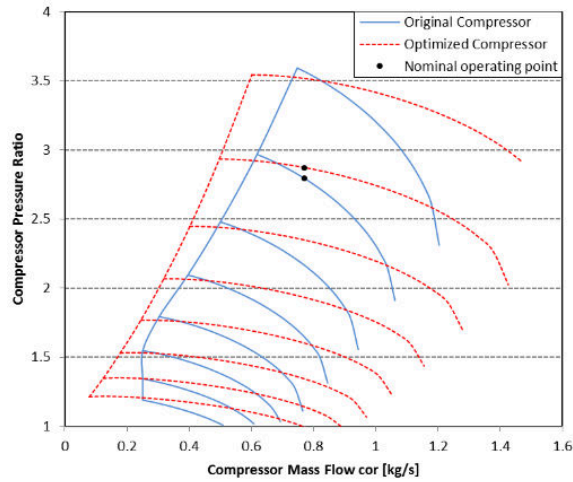


Figure 14: Original and optimized compressor performance map.

With turbocharged diesel engine performance analysis being carried out, optimized compressor operation is calculated. The T/C operating line on optimized compressor performance map is presented in Figure 16. For specific fuel consumption, a 0.27% decrease in nominal operating point is shown in Figure 17. Also a 0.38% reduction in nominal T/C speed occurs, hence positively affects T/C bearings life.

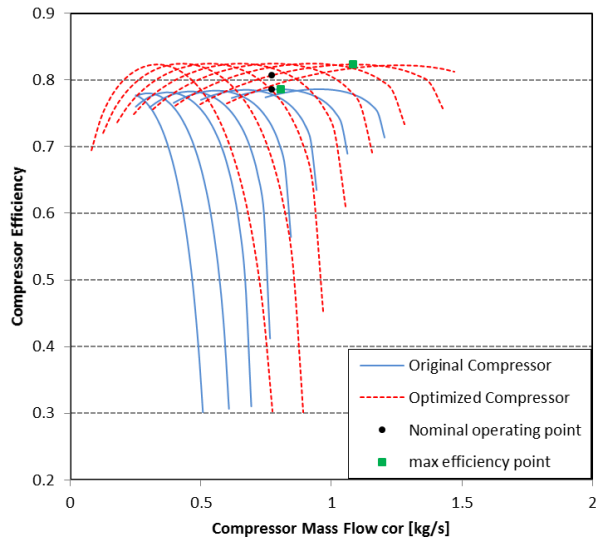


Figure 15: Original and optimized compressor efficiency map.

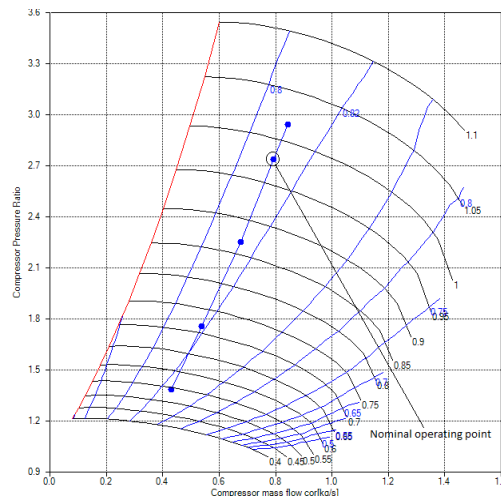


Figure 16: Optimized compressor map and operating line.

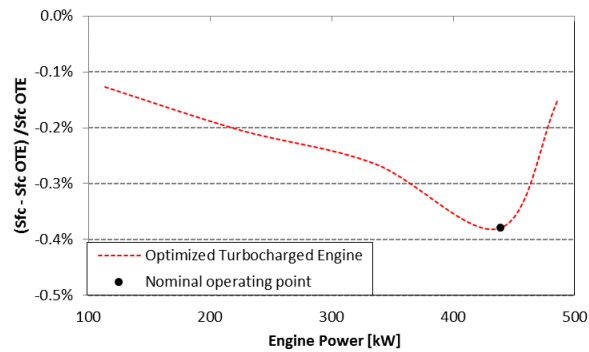


Figure 17: Sfc change for optimized compressor retrofit.

Concluding, the third option provides the best retrofitting solution in relation to first and second one, as Figure 9, Figure 13 and Figure 17 show. Nevertheless, it should be noted that the current option requires compressor component manufacturing, hence increasing the retrofitting cost (CNC wheel milling and shroud/scroll housing rebuild). The cost for high capacity marine centrifugal compressors may exceed the value of 10000\$.

Finally, a CFD analysis has to be carried out, as a mean of validating the compressor optimization tool capability to capture the performance trends based on geometry variation by comparing the pressure ratio and efficiency between CFD and corresponding 1D method.

Platform mode 2 CFD Validation

For compressor optimization (mode 2) validation, steady-RANS simulation is performed for both original and optimized compressors. Specifically, a CFD analysis is carried out, in order to validate the pressure ratio and efficiency trends as obtained by the corresponding 1D model.

The current simulations are conducted within ANSYS CFX 17.0. For computation time reduction, a single passage simulation is applied, knowing that during stable operation, the flow can be assumed as periodic. Centrifugal compressor domain consists of two domains, impeller and diffuser. Impeller mesh size is approximately 2 millions, succeeding mesh size independence, and diffuser size 140000. Both components achieve a maximum y^+ level lower than 2.58.

For CFD model validation, the NASA B30-D2 vaneless diffuser centrifugal compressor [19] is considered. This is a transonic compressor, which was studied as both vaned and vaneless diffuser with a NASA in-house CFD code. Between both of them, the vaneless diffuser compressor is chosen as more relative to the current work. The maximum error is about (0.5%) for the efficiency curve at nominal speed, the only available as reference. The comparison is shown in Figure 18.

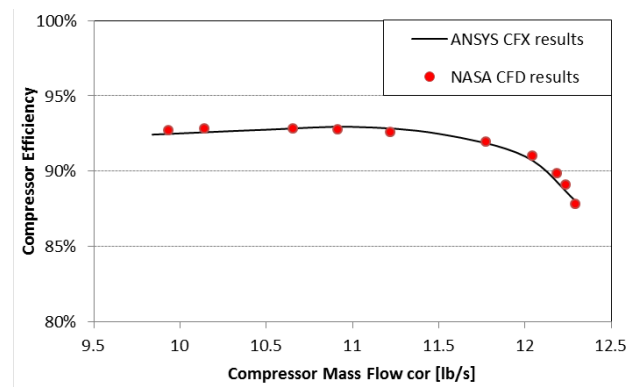


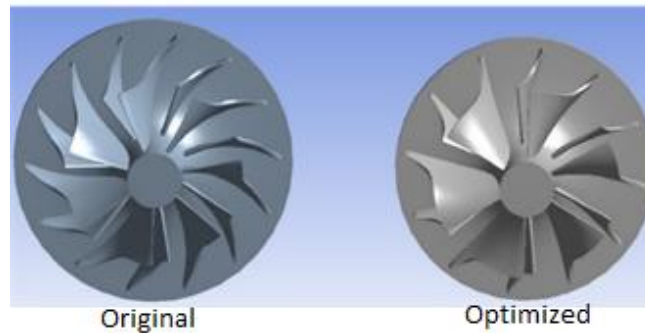
Figure 18: CFD compressor model validation [19].

For creating a 3D geometry for original and optimized compressor, a transformation from 1D to 3D geometry technique is developed in the context of the present work. Basically, it is a blade angle/thickness adaptation based on NASA B30-D2 3D compressor data. The correlations of this technique are presented below.

$$k_1(S) = \frac{f(S)}{f(0)} g_{le} \quad k_2(S) = \frac{f(S)}{f(1)} g_{te} \quad (2)$$

$$g(M) = \begin{cases} k_1(S) & , \quad S = 0 \\ S k_1(S) + (1 - S) k_2(S) & , \quad S = (0,1) \\ k_2(S) & , \quad S = 1 \end{cases} \quad (3)$$

The parameter S is the dimensionless distance between blade leading and trailing edge. Thus, for leading edge is equal to zero and for trailing edge is equal to one. The f function represents the NASA B30-D2 blade data (angle and thickness) for each blade position and g function the adopted blade data according to given leading and trailing edge blade data (g_{le} and g_{te}). Having calculate blade angle and thickness across blade for span (0, 0.5, 1) for original and optimized compressor and combining them with the corresponding 1D geometry, a 3D geometry can easily be generated for each compressor (Figure 19).

**Figure 19: Compressors 3D geometry generation.**

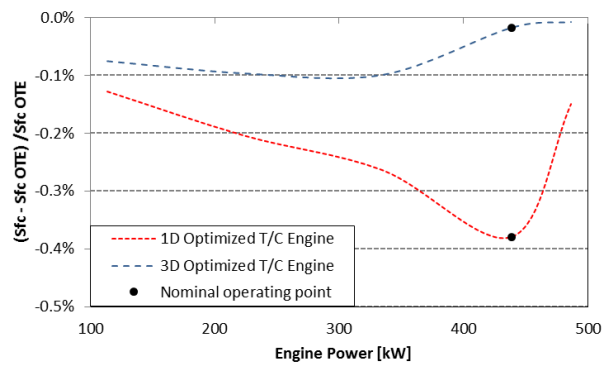
Then, a CFD simulation is carried out at the nominal operational point, according to original turbocharged diesel engine shop trials for both geometries.

The pressure ratio and efficiency trends as obtained by 1D model and CFD simulation, in the nominal operation point are shown in Table 4. It can be seen that the 1D model is able to capture the performance trend based on geometry variation, hence making it a reliable tool during 1D design.

Table 4: Comparison between 1D model and CFD.

Parameter	1D model	CFD
Total Pressure Ratio	+12.39%	+14.91%
Compressor Efficiency	+2.1%	+1.3%

Specifically, the efficiency trend between original and optimized compressor shows a small difference between 1D and CFD model, with a value about 0.8%. For pressure ratio the difference increases to 2.52% which is expected due to the nature of single zone model. The map generated from the 3D geometry shows a 0.02% reduction in SFC for the nominal operating point that is slightly less than the value estimated using the 1D map (Figure 20).

**Figure 20: Sfc change comparison between 1D and 3D geometry.**

Using indicative costs about T/C purchase [20], centrifugal compressor (one part order) impeller CNC milling and scroll housing casting, Figure 21 shows the payback period for each option. Fuel costs typical at the period of writing this paper have been employed (marine diesel fuel cost (bunker) varies and data for different fuels and locations are published daily, as for example in [21]).

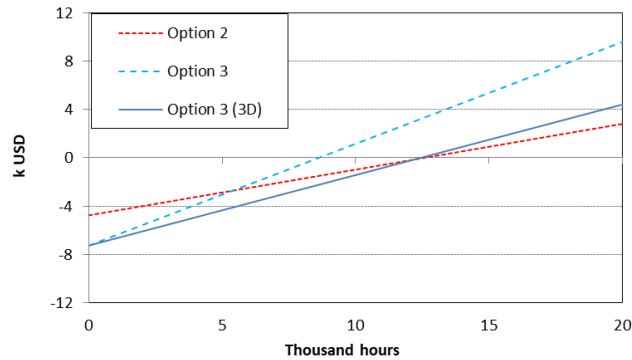


Figure 21: Estimated cumulative benefit in function of time of operation.

For our test case, under the assumptions used, the payback period for option 2 is 12574h and for option 3 is 8621h. Taking into consideration, the compressor performance reduction for transforming geometry from 1D to 3D, the new payback period is about 12441h. Option 3 seems to be the best choice (even with this reduction), having the shortest payback time.

SUMMARY-CONCLUSION

A marine turbocharger retrofitting platform, presented in this work, utilizes 1D models for calculating the turbomachinery components maps and a fully coupled process integrating the turbomachinery components and the diesel engine. Having two modes of operation, it allows the T/C retrofitting process to become fully automatic.

In the first mode, all available turbo-components (compressors and turbines) are examined in order to select the one that match the entire engine system while retaining or improving the diesel engine efficiency. Also a manual flow trimming tool is integrated in order to adapt the turbocharger performance to satisfy the engine operation requirements.

In the second mode, an optimization procedure is followed, in order to redesign the compressor to match the entire system in an optimum way. Taking advantage from the usage of dimensionless parameters as optimization variables with defined range, it can provide a more robust, faster converging and fully automatic procedure, using the compressor mass flow, the external power and the rotational speed in nominal operation point as input data. Both input data and the speed restriction are available in shop trials data, hence not requiring the original compressor geometry and performance measuring.

Then, the platform is applied in real retrofitting case study where three retrofitting options are analyzed (compressor retrofit, whole turbocharger retrofit and compressor redesign). In the first and second option, by utilizing the platform first mode, a turbocharger retrofit is performed, using the corresponding available turbo-components. The solutions, that the platform provides, show that the initial performance cannot be achieved using off-the-self solutions, having a specific fuel consumption increase about 0.8% for option one and 0.27% for option two in nominal operation point. For third option (second mode usage) a compressor designing is performed, providing an improved retrofitting solution, aiming to at least reconstituting the original diesel engine

performance, certified during shop-trials. For optimized compressor a 2% efficiency increase in nominal operating point is noticed in relation to original one.

Thus, the entire diesel engine system efficiency improvement is succeeded, leading to a sfc decrease about 0.27%. A CFD analysis is carried out, comparing the pressure ratio and efficiency between CFD and corresponding 1D method. A 0.8% increase in efficiency trend and a 2.52% in pressure ratio trend are noticed, showing that 1D model is a reliable tool during 1D design.

Retrofit process relying on engineers' personal judgment may not be optimal and thus a turbocharged marine diesel engine unnecessary degradation occurs. This degradation leads to an engine fuel consumption increase, hence NO_x and CO₂ increase. With the mass usage of the platform proposed here, it is guaranteed that the retrofit process, will provide the best retrofit solution, leading to a NO_x and CO₂ decrease. Both gases are responsible for climate change and global warning. Also the usage of the platform will increase the productivity of turbocharger manufacturers, decreasing the time, spending in tasks such as, searching for available turbochargers, matching analyzing and designing a new compressor.

The optimization technique using dimensionless parameters presented in the current work, can be a reliable tool during 1D compressor design, in case of no available initial geometry. Also, 1D to 3D transformation technique, developed in the context of the present work, can provide a good 3D geometry in case of no available 3D optimization, or a proper initial geometry for 3D optimization.

These elements of the approach proposed here and the fact that it does not need proprietary information, constitute novel features that to the authors' knowledge cannot be found in previously published works.

ACKNOWLEDGEMENTS

The authors are grateful to acknowledge Mr Yiannis Paraskevopoulos and Turbomed SA for providing the turbocharger data used in this study. The authors would also like to appreciate ANSYS Inc for the use of their CFD software and their technical support during this program of research.

REFERENCES

- [1] Bricknel, D., "Marine Gas Turbine Propulsion System Application." *Proceeding of ASME Turbo Expo*. GT2006-90751. Barcelona, Spain, , May 8-11, 2006.
- [2] Button, R. W., Martin, B., Sollinger, J. and Tidwell, A., "Assessment of Surface Ship Maintenance Requirements." RAND Corporation,, Santa Monica, Calif (2015).
- [3] Watson N. and Janota M. S., "Turbocharging the Internal Combustion Engine.", Macmillan press ltd, London (1982).

- [4] Galvas, M.R., "Fortran program For predicting off design performance of Centrifugal Compressor." Technical Report No. TN D-7487. NASA Lewis Research Center, Cleveland, Ohio. 1973.
- [5] Aungier, R. H., "Mean streamline aerodynamic performance analysis of centrifugal compressor." ASME Journal of Turbomachinery. Vol 117 No 3 (1995):pp. 360-366.
- [6] Rodgers, C, "Typical Performance Characteristics of Gas Turbine Radial Compressors." ASME Journal of Eng. Power. Vol. 86 No. 2 (1964) :pp. 161-170.
- [7] Japikse, D, "Centrifugal Compressor Design and Performane." Concepts ETI Inc:Wilder,, Wilder VT, USA (1996).
- [8] Stuart, C.,Spence, S.,Filsinger, D., Starke A. and Kim, S. I., "Characterising the influence of impeller exti recirculation on Centrifugal Compressor work input." *Proceeding of ASME Turbo Expo. GT2017-63047*. Charlotte, NC, USA,, June 26 - 30 , 2017.
- [9] Stuart, C., Spence, S., Filsinger, D., Starke, A. and Kim S., "A three-zone modelling approach for centrifugal compressor slip factor prediction." *Proceeding of ASME Turbo Expo. GT2018-75324*. Oslo, Norway,, June 11-15, 2018.
- [10] Rossetti, A., Ardizzon, G., Pavesi, G. and Cavazzini, G., "An optimum design procedure for an aerodynamic radial diffuser with incompressible flow at different Reynolds numbers,." *Imeche Journal of Power and Energy*, Vol. 224 (2010): pp. 69–84.
- [11] Li, P., Gu, C. and Song, Y., "A New Optimization Method for Centrifugal Compressors Based on 1D Calculations and Analyses." *Energies Journal* Vol. 8 No. 5, (2015): pp. 4317-4333.
- [12] Ntonas, K. ,Aretakis, N. , Roumeliotis, I., Pariotis, E., Paraskevopoulos, Y. and Zannis T. , "Integrated Simulation Framework for Assessing Turbocharger Fault Effects on Diesel Engine Performance and Operability." *ASCE Journal of Energy Engineering* (2020). (accepted, to be published in 2020).
- [13] Wasserbauer, C.A. and Glassman, A. J., "Fortran Program for predicting off-design performance of Radial-Inflow Turbines." Technical Report No. TN D-8063. NASA Lewis Resedrcb Center, Cleveland, Ohio. 1975.
- [14] Turbomed SA., "Turbo, Technology, World care." Athens, Greece, www.turbomed.gr.
- [15] Emara, K., Emara, A. and Razeq, E. S. A., "Turbocharger selection and matching criteria in a heavy duty diesel engine." *Journal of Scientific & Engineering Research*, Vol. 7 No 12 (2016): pp. 609-615.
- [16] Swain,D., and Engeda, A., "Effect of Impeller blade trimming on the performance of a 5,5:1 pressure ratio centrifugal compressor." *Imeche Journal of Power and Energy* Vol 228 (2014): pp. 878–888.
- [17] Shepherd, D. G., "Principles of Turbomachinery." MacMillan and Co LTD, New York, (1956)..

- [18] Antonakis, A., Nikolaidis, T., & Pilidis, P., “Multi-Objective Climb Path Optimization for Aircraft/Engine Intergration Using Particle Swarm Optimization” *Journal of Applied Sciences* Vol 7 No. 5 (2017): pp. 1-22
- [19] Medic G., Sharma, O. P. ,Jongwook, J., Hardin, L. W., McCormick, D. C., Cousins, W. T., Lurie, E. A., Shabbir, A. , Holley,B. M., and Van Slooten, P. R. “High Efficiency Centrifugal Compressor for Rotorcraft Applications.” Technical Report No. NASA/CR—2014-218114/REV1. NASA Langley Research Center, Hampton, Virginia. 2014.
- [20] Alibaba.com., “Catalog: Auto Engine -other auto engine parts.” https://www.alibaba.com/catalog/other-auto-engine-parts_cid100003861?spm=a2700.details.debelsubf.6.41022ffaXZXJy9.
- [21] Ship & Bunker., “News and intelignce for the marine fuels industry.” www.shipandbunker.com.
- [22] Wiesner, F.J., “A Review of Slip Factors for Centrifugal Impellers.” *ASME Journal of Eng. Power* Vol 89 (1967): pp. 558–572.

APPENDIX: PRE-PROCESSOR PROCEDURE

The following mathematical procedure is following in the preprocessor, to transform dimensionless parameters (Table 1) into 1D geometry. This transformation is accomplished by using compressor mass flow (\dot{m}) and external power (Pwr_{turb}) as input data. A zero inducer incidence angle is forced ensuring that the design point is not close to surge or choke line.

For the given turbine output power, the required compressor power is calculated by the following equation:

$$Pwr_{comp} = \eta_{C,Ex} Pwr_{turb} n_m$$

For the power transmission from the turbine to compressor the turbo cartridge mechanical losses are set 95%. Parasitic efficiency $\eta_{C,Ex}$ is defined as follows:

$$\eta_{C,Ex} = \frac{Dh_{comp}}{Dh_{comp} + Dh_{comp,RC} + Dh_{comp,DF}}$$

It is taken equal to 1 for the first iteration.

Impeller outlet total temperature is computed for a certain inlet total temperature and compressor power.

$$T_{t2} = \frac{Pwr_{comp}}{\dot{m} C_p} + T_{t1}$$

Knowing the demanded mass flow rate, impeller power and specific speed, an initial guess of density (ρ_1) is made to calculate the impeller rotational speed.

$$\omega = 2 \pi \frac{Ns}{\sqrt{\frac{\dot{m}}{\rho_1}}} \left(\frac{Pwr_{comp}}{\dot{m}} \right)^{\frac{3}{4}}, \quad N = \frac{30 \omega}{\pi}$$

Additionally, the slip factor is estimated based on Wiesner formula [22]. The following equations allow the calculation of blade speed and circumferential speed in impeller outlet for a given blade backsweep angle and flow coefficient in impeller outlet.

$$U_2 V_{U2} = \frac{Pwr_{comp}}{\dot{m}}, \quad \frac{V_{U2}}{U_2} = \sigma(1 - \Phi_2 \tan[\beta_2])$$

Having calculated exducer blade velocity and having flow coefficient as input data, the impeller outlet radial velocity and radius are found.

$$V_{R2} = \Phi_2 U_2, \quad R_2 = \frac{U_2}{\omega}$$

Blade speed, inducer axial velocity and the impeller inlet blade angle in mid span are then calculated:

$$U_{1m} = \omega R_{1m}, \quad V_{a1} = \frac{\dot{m}}{\rho_1 * A_1}, \quad \beta_{1m} = \text{atan}(U_{1m}/V_{a1})$$

Static inlet temperature and pressure are calculated in order to predict the air density in inlet. Then the process from equation is repeated from blade speed calculation until density converges to a value.

$$T_{s1} = T_{t1} - \frac{V_{a1}^2}{2 C_p}, \quad P_{s1} = P_{t1} \left(\frac{T_{s1}}{T_{t1}} \right)^{\frac{\gamma}{\gamma-1}}, \quad \rho_1 = \frac{P_{s1}}{R_{GAS} T_{s1}}$$

The impeller outlet density can be found considering the calculated velocity triangle and static conditions at exducer position.

$$T_{s2} = T_{t2} - \frac{V_{R2}^2 + V_{U2}^2}{2 C_p}, \quad P_{s2} = P_{t2} \left(\frac{T_{s2}}{T_{t2}} \right)^{\frac{\gamma}{\gamma-1}}, \quad \rho_2 = \frac{P_{s2}}{R_{GAS} T_{s2}}$$

Impeller outlet area, hence exducer blade length, can then be evaluated.

$$A_2 = \frac{\dot{m}}{\rho_2 V_{r2}}, \quad b_2 = \frac{A_2}{2 \pi R_2}$$

For the vaneless diffuser calculations, it is considered that diffuser passage width is equal to blade length.

At first, it is assumed that in vaneless diffuser only pressure drop exists. In the first iteration, P_{dl} is set as zero. Then the mean line code calculates the pressure drop, correcting it.

$$P_{t3} = P_{t2} - P_{dl}, \quad T_{t3} = T_{t2}$$

In order to calculate vaneless diffuser outlet absolute velocity, T_{s3} and C_3 have to be calculated.

$$T_{s3} = T_{t3} \left(1 + \frac{\gamma-1}{2} MN_3^2 \right), \quad C_3 = \sqrt{\gamma R_{GAS} T_{s3}}$$

With C_3 calculated, V_3 and static pressure at position 3 can be easily computed.

$$V_3 = MN_3 * C_3 \quad , \quad P_{s3} = P_{t3} \left(\frac{T_{s3}}{T_{t3}} \right)^{\left(\frac{\gamma}{\gamma-1} \right)}$$

Since static conditions in diffuser outlet have been computed while flow angle is known from impeller velocity triangle, density diffuser outlet radius can then be allocated.

$$\rho_3 = \frac{P_{s3}}{R_{GAS} T_{s3}}, \quad A_3 = \frac{\dot{m}}{V_{r3} \rho_3}, \quad R_3 = \frac{A_3}{2 \pi b_3} = \frac{A_3}{2 \pi b_2}$$

Having computed an initial 1D geometry, then the mean line code predicts the compressor adiabatic η_{AD} and parasitic efficiency $\eta_{C,EX}$ for the given mass flow. The above described calculations are then repeated for an improved estimation. The one iteration choice is made, since it was observed that additional iterations do not offer a significant improvement.